

# Vessel Segmentation and Tracking Using a Two-Dimensional Model

M. J. Cree<sup>1</sup>, D. Cornforth<sup>2</sup> and H. F. Jelinek<sup>3</sup>

<sup>1</sup>Department of Physics and Electronic Engineering, University of Waikato, Hamilton.

<sup>2</sup>School of Environmental and Information Sciences, Charles Sturt University, Albury, Australia.

<sup>3</sup>School of Community Health, Charles Sturt University, Albury, Australia.

Email: m.cree@ieee.org

## Abstract

The segmentation and analysis of blood vessels in retinal images is of immense interest for study of diseases involving vasculature changes. An algorithm to segment blood vessels in colour retinal images by tracking of vessels is described. This algorithm proceeds by fitting a physically inspired two-dimensional model of the vessel profile to a local region of the vessel. By fitting in this manner a number of parameters, such as diameter and orientation, of the local vessel segment, can be accurately measured as tracking proceeds. A modification to the model that enables tracking of tortuous vessels is described. A method to detect vessel branches is also described. Illustrations of the vessel tracking working on retinal images are given.

**Keywords:** retinal imaging, vessel tracking

## 1 Introduction

Analysis of the retinal vessel structure is of immense interest for the investigation of diseases that involve structural or functional changes in the vasculature. Changes in retinal vasculature, such as haemorrhages, angiogenesis, increases in vessel tortuosity, blockages and arteriolar-venular diameter ratios are important indicators of, for example, diabetic retinopathy, retinopathy of prematurity and cardiovascular risk.

There is a growing body of literature on the segmentation of blood vessels from retinal images. The vast majority of the literature is based on physically inspired models of vessel appearance, and somewhat dependent on the imaging modality. For example, in fluorescein angiography the vessels appear bright (hyperfluorescent), whereas in red-free imaging the vessels appear dark compared to the retina bed. Vessel segmentation algorithms can be coarsely divided into two classes: those that are pixel operator based, and those that track vessels in a local region. The first class involve operators, such as morphological operators, that are applied globally to the whole image, whereas the second class, once it has a point on the vessel only needs to analyse the local region about the vessel to track the vessel through the image.

Pixel operator methods are characterised by convolution methods using a kernel that is a model of the vessel appearance [1, 2], threshold probing [3], morphological operators [4, 5], wavelets [6], preprocessing combined with region growing [7] and

preprocessing combined with artificial intelligence applied to pixel classification [8, 9, 10]. A review of retinal vessel segmentation algorithms can be found in [11] and comparative tests of some pixel based segmentation algorithms can be found in [12, 13, 14].

Most vessel tracking or tracing methods, once given an initial point on the vessel, estimate the vessel width and orientation within a local region about the current point. Then a small step is taken in the direction of the vessel orientation and the procedure is repeated until the full vessel is traced out. Methods of estimating the vessel width and orientation at the current location vary. Some proceed by detecting the edges of the vessel closest to the current point to estimate the orientation [15]. These can suffer from substantial error if an insufficient number of pixels about the edges are used. To improve on this, some apply convolution operators, either using a model of the vessel shape itself, or two separate operators modelling the vessel edges in the neighbourhood of the vessel edges [16]. By applying the convolution with the model rotated to different orientations, the peak response can be used to more accurately measure vessel orientation.

This suggests a better way of estimating vessel orientation and width within a local region. Rather than applying a number of convolutions at various orientations one could fit a model of the vessel with an optimisation procedure, such as a non-linear least squares fit. By using a two-dimensional

local region about the current point a very accurate estimate both of vessel width and vessel orientation can be made. Provided the vessel is not too tortuous (i.e. it does not change profile or orientation within the local region) then the two-dimensional fit should have much better success thus stepping in the correct direction is better guaranteed. Furthermore, because a reasonable number of pixels can be used in the fit, vessels in noisy images or in low-contrast regions can be tracked.

In the following we describe a vessel tracking algorithm based on the fitting of a two-dimensional physically inspired model to a local region about the vessel. Section 2 gives an overview of physically inspired models for vessel tracking. In section 3 the tracking algorithm is described. In addition to describing tracking by two-dimensional non-least squares fitting in a local region, we also describe a modification to the model that improves the tracking of vessels in the presence of some vessel tortuosity. Following that, in section 3.1 an algorithm to detect vessel branches is described. An example of the algorithm running on a retinal image is given as evidence of its usefulness in section 4.

## 2 Physical Vessel Models

A simple model for blood vessels assumes that the darker appearance of vessels is primarily due to the attenuation of red-free light as it passes through the blood column. Attenuation is according to Bouguer's Law, and the exit beam intensity is given by [17],

$$I(x) = I_0 e^{-\int \alpha(x,z) dz} \quad (1)$$

where  $\alpha(x, z)$  is the linear attenuation coefficient,  $x$  is the dimension in the plane of the retina across the vessel and  $z$  is depth into the retina. Taking  $\alpha$  as constant throughout the vessel, and the vessel profile as symmetric and circular, then to second order the received light is,

$$I(x) = I_0 \left( 1 - a e^{-(x-x_0)^2/2\sigma^2} \right) \quad (2)$$

where  $x_0$  is the centre of the vessel,  $\sigma$  defines the width of the vessel, and  $a$  is a constant giving the relative amount of light absorbed by the vessel.

This model fails to take account of the light reflex often seen in the centre of the vessel. It is often suggested that the light reflex is due to specular reflection from the surface of a smooth column of blood, however a more detailed model by Brinchmann-Hansen and Heier showed that the light reflex is better explained by the scattering of light off the rough column of blood and the intravascular column of erythrocytes [18]. This scattering can also

be usefully modelled by a Gaussian that is narrower and inverted with respect to the simple vessel model. This leads to the double Gaussian model,

$$I(x) = I_0 \left( 1 - a e^{-(x-x_0)^2/2\sigma^2} + b e^{-(x-x_0)^2/2\sigma_r^2} \right) \quad (3)$$

with  $b$  the relative fraction of the light reflex, and  $\sigma_r$  the light reflex width where  $\sigma_r < \sigma$ .

A further proposed model [19] for the light reflex is similar to the above, but instead of adding the two components together, switches between the two components, namely

$$I(x) = \begin{cases} I_0 \left( 1 - a e^{-(x-x_0)^2/2\sigma^2} \right) & x < P, x > Q \\ I_0 b e^{-(x-x_1)^2/2\sigma_r^2} & P \leq x \leq Q \end{cases} \quad (4)$$

for  $a$  and  $b$  are the relative amounts of the two components,  $x_1$  is the centre and  $\sigma_r$  the width of the light reflex, and  $P$  and  $Q$  define the cutover points between the two components.

## 3 2D Vessel Tracking

We track the vessel by fitting in a local region of the vessel a two-dimensional model of the vessel. The 2D model extends the 1D models of section 2 by giving the vessel an orientation in the 2D plane, and extending the vessel in the direction orthogonal to its cross-section. It is assumed that the extension of the vessel is linear and uniform, that is, it has the same cross-section at all points along the vessel (at least on the scale of the local region). Given a point  $(x, y)$  on the vessel, an estimate of orientation  $\theta$ , and an estimate of the vessel width  $\sigma$ , then a small region is cut out about the point and a 2D non-linear least-squares fit of the vessel model is made over the local region. This enables an accurate measurement of vessel width and orientation to be made. Given the width and orientation, then a small step is made in the direction of the vessel orientation, the previous width and orientation are used as new estimates, and a new 2D fit is made to the vessel. Using 2D fits the vessel width and orientation can be estimated accurately, enabling the tracking to proceed reliably.

The generalisation of the model to two-dimensional fitting requires that we consider  $(x, y)$  coordinates of the retina and the orientation  $\theta$  of the vessel with respect to the  $x$ -axis. We construct new coordinates  $(u, v)$  with  $u$  pointing in the same direction as the vessel and  $v$  orthogonal to the vessel, then,

$$\begin{aligned} u &= x \sin \theta - y \cos \theta \\ v &= x \cos \theta + y \sin \theta \end{aligned} \quad (5)$$

with the vessel profile given by the single Gaussian model,

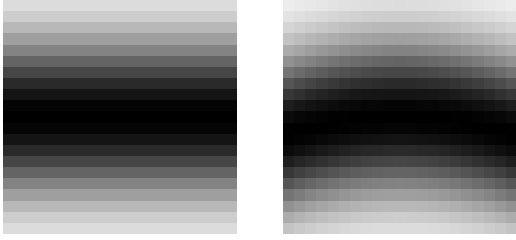


Figure 1: The 2D vessel function for no curvature (left,  $\eta = 0$ ) and with some curvature (right,  $\eta > 0$ ).

$$I(v) = A - Be^{-(v-v_0)^2/2\sigma^2}. \quad (6)$$

Here  $A$  is the background intensity,  $B$  is the contrast of the vessel with respect to the background and  $v_0$  enables the vessel centre to be shifted in the  $v$ -direction.

Occasionally a vessel may be tortuous and bend suddenly in a localised region. This can cause the 2D fitting to fail, as the assumption that the vessel cross-section can be extended linearly in one direction is violated. To account for tortuosity it is advantageous to enable the vessel to flex; this was achieved by adding a quadratic term in  $v$  to  $u$ , that is, by generalising equation 5 to

$$\begin{aligned} u &= x \sin \theta - y \cos \theta + \eta v^2 \\ v &= x \cos \theta - y \sin \theta \end{aligned} \quad (7)$$

where  $\eta$  describes the curvature of the vessel. If  $\eta = 0$  then there is no curvature of the vessel. If  $|\eta| > 0$  then the vessel function will bend in the direction of  $u$  about the origin. In figure 1 is shown the function for  $\eta = 0$  and  $\eta > 0$ . A negative  $\eta$  causes a curvature in the opposite direction.

We use the `nlinfit` routine of Matlab to effect a non-linear least-squares fit of the model to the underlying image data within the local region. It is an implementation of the Levenberg-Marquardt algorithm and only requires specification of the model itself, as it estimates the local gradient of the model by numerical differentiation.

The local region used for fitting is defined by taking  $2 \text{ceil}(2\sigma) + 1$  pixels along the  $u$  axis, and  $2 \text{ceil}(\frac{3}{2}\sigma) + 1$  pixels along the  $v$ -axis as illustrated in figure 2 and figure 5. Our experience agrees with [20] in that the local region for fitting must be oriented with the vessel for reasonable estimation of the vessel width. Nevertheless, the fitting routine has a tendency to over-estimate vessel width if the local region is made too small, and under-estimate vessel width if the local region is made too large. To prevent an oscillation in vessel width resulting during tracking, the vessel width is regulated by replacing the measured vessel width of the current step with the average of itself and that of the previous step.

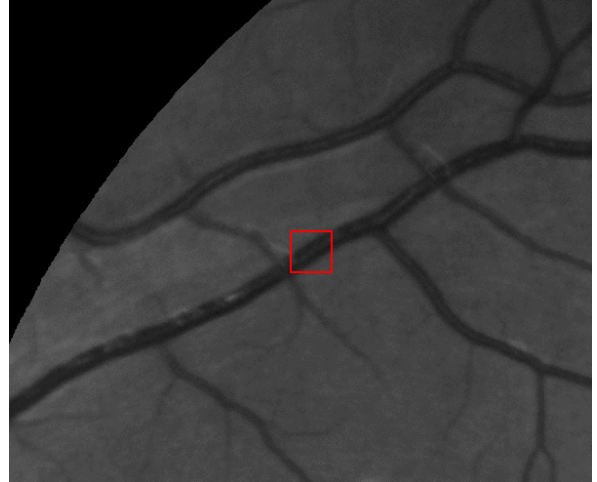


Figure 2: Retinal image (green plane only) with a local region for vessel fitting shown.

Experiments with the additive double Gaussian model (equation 3) proved problematic. Often the fit would diverge to a local minimum with large vessel widths for both Gaussians, that is, the region of convergence of the initial conditions was too restrictive to allow successful tracking. Most of our experimentation is with the single Gaussian model (equation 2), and we have begun experimentation with the switching Gaussian model (equation 4).

### 3.1 Tracking Branches

The vessel tracking algorithm described above is capable of tracking a single vessel even across minor vessel branches and crossing. However, it does not track the actual branches. We describe here an algorithm to determine branches on the side of vessels and initiate tracking on the branches.

Once a single vessel segment has been tracked, then the program ‘walks’ along the vessel stopping at each fitted centre, and looks for branches either side of the vessel. Two regions-of-interest (ROI), of length  $2 \text{ceil}(\frac{5}{2}\sigma) + 1$  and width  $2 \text{ceil}(\sigma) + 1$  are placed just either side of the vessel and oriented parallel to the vessel (see figure 3). The 75th percentile intensity  $f_{75}$  and the standard-deviation in intensity  $f_\sigma$  are measured within each ROI and the ROI is thresholded at  $f_{75} - 2f_\sigma$  retaining pixels less than the threshold. A necessary condition for a branch to be present in the ROI is that a connected component in the thresholded ROI must extend from the top of the ROI to the bottom. In addition the watershed of the ROI is calculated, and a watershed line must extend from the top of the ROI to the bottom. Neither of these two conditions are sufficient on their own, however when combined

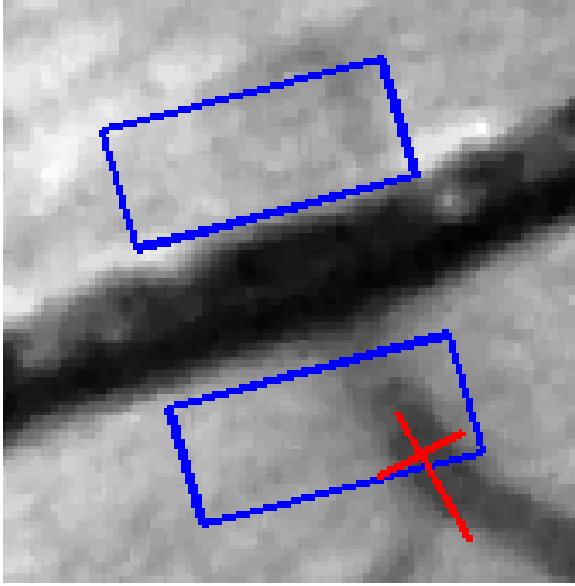


Figure 3: Two ROIs placed about a vessel point with a detected branch shown.

they serve to be very sensitive and quite specific at detecting branches from the vessel.

The above process is repeated along the vessel and new vessel tracking is triggered at the branches. The initial orientation for the branch is estimated from the direction of the watershed line described above, and the vessel width from the appropriate connected component in the thresholded ROI. Tracking and branch detection can then be repeated on a recursive basis. In figure 3 an already tracked vessel is shown with two ROIs placed either side of it. The lower ROI has a vessel branch, for which the detected branch and orientation is shown. The image within this ROI, the thresholding showing the connected component, and the watershed are shown in figure 4.

## 4 Results

A local region of a vessel in a retinal image is illustrated in figure 2, and an example of fitting the model to a vessel in the local region is shown in figure 5. The red (darker) line and cross show the estimated orientation location of the centre of the vessel used to initiate the 2D non-linear least squares fit. The green (lighter) line and cross show the fitted orientation and centre of the vessel, and can be seen to be better oriented and positioned than the red line and cross. A three-dimensional view of the fit is shown in figure 6.

The result of tracking along a vessel is shown in figure 7. The vessel has been successfully tracked past junctions involving branches and also other crossing vessels. The tracking terminated at a clus-

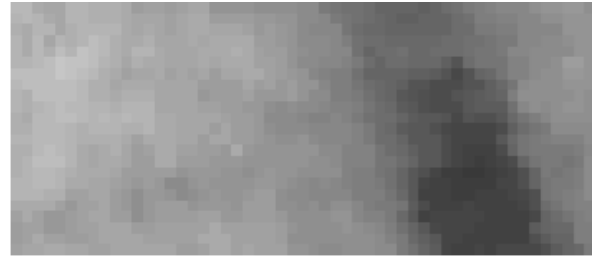


Figure 4: The image intensity (top), the thresholded images (middle) and the watershed (bottom) of the branch in the lower ROI of figure 3.

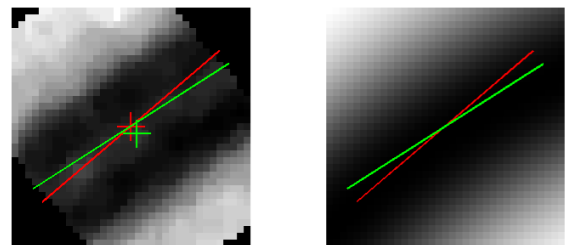


Figure 5: 2D fitting within a local region about a vessel. The red (darker) line and cross are the seed values of orientation and position, and the green (lighter) line and cross are the resultant fitted orientation and position. Left: image data. Right: fitted vessel function.

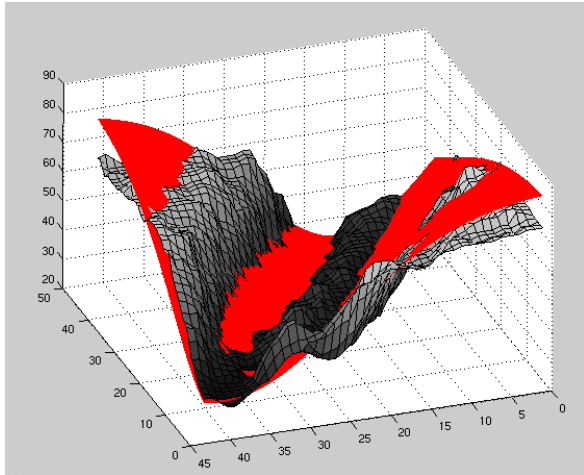


Figure 6: Vessel fit shown as a three-dimensional plot. The smooth curve is the fitted vessel function, and the rough surface is the image data.

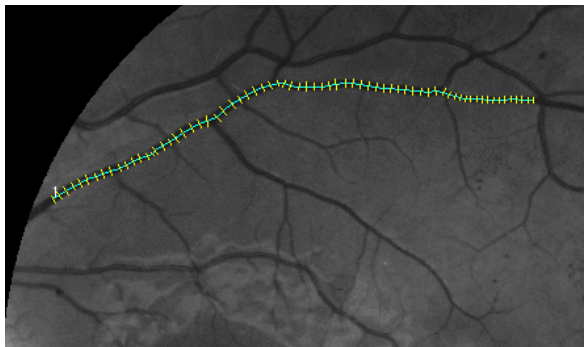


Figure 7: Tracking of a single vessel. The little bars across the vessel show the fitted positions and the measured width of the vessel.

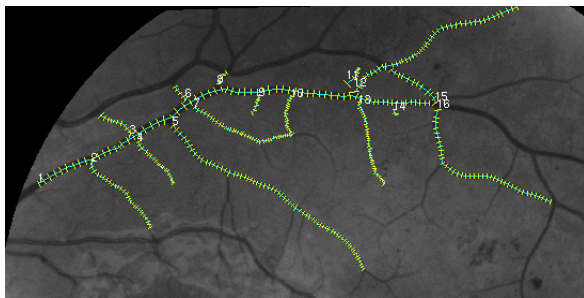


Figure 8: Tracking of a vessel with branches identified and in turn tracked. The initiating points for tracking the branches are numbered.

ter of vessels where it became impossible to fit the model to the vessel.

After tracking the above vessel, checking for branches about the vessel was initiated, and the located branches in turn were tracked. The result is shown in figure 8. All reasonable crossings and branches are tracked. There is one false initiation of tracking (numbered 11).

## 5 Conclusions

The qualitative results shown in this paper are encouraging. We have observed the vessel tracking to be reliable even in the presence of noisy images or poor contrast. With the addition of the flexible model, vessel tracking of tortuous vessels was made possible. The vessel tracking, as described in this paper, sometimes can fail to track on blood vessels that have substantial central reflex. This failure either expresses itself in complete failure to track at all, or the tracking ends up tracking on one side of the vessel, thereby generating erroneous vessel width measures. Preliminary investigations indicate that the switching double Gaussian model of [19] will solve this problem.

In this paper we have discussed the tracking of blood vessels and the detection and subsequent tracking of branches. No mention has been made of how the tracking might be initiated. For this it is necessary to identify a point on a vessel and give the tracking algorithm an estimated vessel diameter and orientation. In a companion paper we describe a system for detecting the optic disc, and initiating vessel tracking in the vicinity of the optic disc.

## Acknowledgements

MJC thanks Charles Sturt University for hosting him while this work was undertaken. HFJ is in receipt of funding from the Diabetes Australia Society. Retinal images were kindly provided by the Waikato Eye-Screening Programme, and the Eye Research Centre, University of Melbourne.

## References

- [1] S. Chaudhuri, S. Chatterjee, N. P. Katz, M. Nelson, and M. H. Goldbaum, "Detection of blood vessels in retinal images using two-dimensional matched filters," *IEEE Trans. Med. Im.*, vol. 8, pp. 263–269, 1989.
- [2] A. Hoover, V. Kouznetsova, and M. Goldbaum, "Locating blood vessels in retinal images by piecewise threshold probing of a matched filter response," *IEEE Trans. Med. Im.*, vol. 19, pp. 201–210, 2000.
- [3] X. Y. Jiang and D. Mojon, "Adaptive local thresholding by verification-based multi-threshold probing with application to vessel detection in retinal images," *IEEE Trans. Pat. Anal. Mach. Int.*, vol. 25, no. 1, pp. 131–137, 2003.

- [4] B. Fang, W. Hsu, and M. L. Lee, "Reconstruction of vascular structures in retinal images," in *International Conference on Image Processing (ICIP2003)*, vol. 2, pp. 157–160, 2003.
- [5] F. Zana and J. C. Klein, "Segmentation of vessel-like patterns using mathematical morphology and curvature evaluation," *IEEE Trans. Im. Proc.*, vol. 10, no. 7, pp. 1010–1019, 2001.
- [6] R. M. Cesar, Jr and H. F. Jelinek, "Segmentation of retinal fundus vasculature in nonmydriatic camera images using wavelets," in *Angiography and Plaque Imaging* (J. S. Suri and S. Laxminarayan, eds.), pp. 193–224, Boca Raton, FL: CRC, 2003.
- [7] M. E. Martínez-Pérez, A. D. Hughes, A. V. Stanton, S. A. Thom, A. A. Bharath, and K. H. Parker, "Segmentation of retinal blood vessels based on the second directional derivative and region growing," in *IEEE International Conference in Image Processing (ICIP'99)*, (Kobe, Japan), pp. 173–176, 1999.
- [8] R. Nekovei and Y. Sun, "Back-propagation network and its configuration for blood vessel detection in angiograms," *IEEE Trans. Neur. Netw.*, vol. 6, no. 1, pp. 64–72, 1995.
- [9] J. Staal, M. D. Abramoff, M. Niemeijer, M. A. Viergever, and B. van Ginneken, "Ridge-based vessel segmentation in color images of the retina," *IEEE Trans. Med. Im.*, vol. 23, no. 4, pp. 501–509, 2004.
- [10] K. A. Vermeer, F. M. Vos, H. G. Lemij, and A. M. Vossepoel, "A model based method for retinal blood vessel detection," *Comput. Biol. Med.*, vol. 34, no. 3, pp. 209–219, 2004.
- [11] K. H. Fritzsche, A. Can, H. Shen, C. L. Tsai, J. N. Turner, H. L. Tanenbaum, C. V. Stewart, and B. Roysam, "Automated model-based segmentation, tracing, and analysis of retinal vasculature from digital fundus images," in *Angiography and Plaque Imaging: Advanced Segmentation Techniques*, Biomedical Engineering Series, pp. 225–297, Boca Raton, FL: CRC, 2003.
- [12] G. Tang and M. J. Cree, "Detection of retinal blood vessels in colour fundus images," in *Proceedings Image and Vision Computing New Zealand 2004*, (Akaroa, New Zealand), pp. 1–6, 2004.
- [13] M. J. Cree, J. J. G. Leandro, J. V. B. Soares, R. M. Cesar, Jr, G. Tang, H. F. Jelinek, and D. J. Cornforth, "Comparison of various methods to delineate blood vessel in retinal images," in *Proceedings of the 16th National Congress of the Australian Institute of Physics*, (Canberra, Australia), 2005.
- [14] M. Niemeijer, J. Staal, B. van Ginneken, M. Loog, and M. D. Abramoff, "Comparative study of retinal vessel segmentation methods on a new publicly available database," *Proceedings of the SPIE*, vol. 5370, pp. 648–656, 2004.
- [15] X. W. Gao, A. Bharath, A. Stanton, A. Hughes, N. Chapman, and S. Thom, "Quantification and characterisation of arteries in retinal images," *Comput. Meth. Prog. Biomed.*, vol. 63, pp. 133–146, 2000.
- [16] O. Chutatape, L. Zheng, and S. M. Krishman, "Retinal blood vessel detection and tracking by matched gaussian and kalman filters," in *Proceedings of the 20th International Conference of the IEEE Engineering in Medicine and Biology Society*, vol. 6, pp. 3144–3149, 1998.
- [17] X. Gao, A. Bharath, A. Hughes, A. Stanton, and et al., "Towards retinal vessel parameterisation," in *Proceedings of SPIE International Symposium on Medical Imaging*, vol. 3034, pp. 734–744, 1997.
- [18] O. Brinchmann-Hansen and H. Heier, "Theoretical relations between light streak characteristics and optical properties of retinal vessels," *Acta Ophthalmol.*, vol. 179, pp. 33–37, 1986.
- [19] H. Li, W. Hsu, M. L. Lee, and T. Y. Wong, "Automatic grading of retinal vessel caliber," *IEEE Trans. Biomed. Eng.*, vol. 52, no. 7, pp. 1352–1355, 2005.
- [20] J. Lowell, A. Hunter, D. Steel, A. Basu, R. Ryder, and R. L. Kennedy, "Measurement of retinal vessel widths from fundus images based on 2-D modeling," *IEEE Trans. Med. Im.*, vol. 23, no. 10, pp. 1196–1204, 2004.